Analysis of semileptonic *B* decays in the relativistic quark model

D. Ebert

Institut für Physik, Humboldt-Universität zu Berlin, Newtonstr. 15, D-12489 Berlin, Germany

R. N. Faustov and V. O. Galkin

Institut für Physik, Humboldt-Universität zu Berlin, Newtonstr. 15, D-12489 Berlin, Germany
and Dorodnicyn Computing Centre, Russian Academy of Sciences, Vavilov Str. 40, 119991 Moscow, Russia

We present the new analysis of the semileptonic *B* decays in the framework of the relativistic quark model based on the quasipotential approach. Decays both to heavy $D^{(*)}$ and light $\pi(\rho)$ mesons are considered. All relativistic effects are systematically taken into account including contributions of the negative-energy states and the wave function transformation from the rest to moving reference frame. For heavy-to-heavy transitions the heavy quark expansion is applied. Leading and subleading Isgur-Wise functions are determined as the overlap integrals of initial and final meson wave functions. For heavy-to-light transitions the explicit relativistic expressions are used to determine the dependence of the form factors on the momentum transfer squared. Such treatment significantly reduces theoretical uncertainties and increases reliability of obtained predictions. All results for form factors, partial and total decay rates agree well with recent experimental data and unquenched lattice calculations. From this comparison we find the following values of the Cabibbo-Kobayashi-Maskawa matrix elements: $|V_{cb}| = (3.85 \pm 0.15 \pm 0.20) \times 10^{-2}$ and $|V_{ub}| = (3.82 \pm 0.20 \pm 0.20) \times 10^{-3}$, where the first error is experimental and the second one is theoretical.

I. INTRODUCTION

The investigation of the semileptonic decays of heavy *B* mesons is an important source for the determination of the parameters of the standard model, such as Cabibbo-Kobayashi-Maskawa (CKM) matrix elements V_{cb} and V_{ub}. They also provide valuable insight in quark dynamics in the nonperturbative domain of QCD. Recently significant experimental progress has been achieved in studying exclusive semileptonic *B* decays (for a recent review see, e.g., Ref. [1]). Very important information on both the values of the total decay rates and the differential decay-rate dependence on the momentum transfer is becoming available. The experimental accuracy is constantly increasing due to the large data accumulated at *B* factories. For most decay modes experimental errors are comparable to or already smaller than theoretical ones. Thus the accurate extraction of the CKM matrix elements from the semileptonic *B* decays requires an increase in the reliability and precision of theoretical methods for determining weak decay form factors. Main theoretical approaches for calculating these form factors are lattice QCD, QCD sum rules, and constituent quark models. Unfortunately, the first two approaches are applicable only in limited regions: lattice QCD gives reliable results for high values of the square of momentum transfer from the parent to daughter hadron q^2, while QCD sum rules are suitable only for low q^2. Thus extrapolations for the full q^2 region are at the present inevitable in these methods. On the other hand, quark models, which are not straightforwardly related to QCD (at least this relation is not currently established), allow to determine weak form factors in the whole kine-matical range. To give a correct description of semileptonic decays such models should consistently and comprehensively account for relativistic effects and use the wave functions which lead to correct meson masses. They should also respect all the relations imposed by the symmetries of the QCD Lagrangian arising in the heavy quark limit.

From a theoretical point of view the simplest semileptonic *B* decays are heavy-to-heavy transitions such as $B \rightarrow D^{(*)}e\nu$. The presence of the heavy quark both in the initial and final mesons significantly simplifies the understanding of such processes. The heavy quark limit $m_Q \rightarrow \infty$ is a good initial approximation [2]. In this limit heavy quark symmetry emerges substantially reducing the number of independent characteristics which are necessary for the description of heavy-light meson properties [3]. Mass and spin decouple from the consideration and all meson properties are determined by the light quark degrees of freedom alone. This leads to symmetry relations between form factors responsible for the heavy-to-heavy weak transitions. Thus one needs considerably less independent functions. For the semileptonic *B* decay to the ground state $D^{(*)}$ meson all form factors can be expressed through one Isgur-Wise function [2] which is normalized to 1 at the point of zero recoil of the final meson. However, in reality *b* and *c* quarks are not infinitely heavy and therefore the corrections in inverse powers of the heavy quark mass m_Q (especially m_c) are important. Heavy quark effective theory (HQET) [4] is the adopted tool for a systematic expansion of weak decay amplitudes in $1/m_Q$. The coefficients in this expansion are functions of the velocity transfer in the weak decay and do not depend on spin and flavor of the

heavy quarks. These functions originate from the infrared (nonperturbative) region of QCD and thus cannot be determined from first principles of QCD at the present. It is necessary to use some model assumptions in order to calculate these functions. Note that notwithstanding heavy quark symmetry violation already in the first order in $1/m_Q$, its remnants remain and thus HQET significantly restricts the structure of $1/m_Q$ corrections. E.g., in the first order in $1/m_Q$ for B decays to the ground state $D^{(*)}$ mesons one mass parameter and four additional functions (two of which are normalized at the zero recoil point) emerge instead of 12 possible ones. This is the consequence of QCD and heavy quark symmetry. Thus all models which pretend to describe correctly weak heavy-to-heavy transitions should satisfy HQET symmetry relations.

The theoretical description of exclusive semileptonic heavy-to-light B decays, such as $B \to \pi(\rho)e\nu$, represents a more difficult task since the final meson contains light quarks only. The expansion in inverse powers of the b quark mass does not reduce the number of independent form factors. Only relations between semileptonic and rare radiative decays emerge in the heavy b quark limit. It is important to note that in these decays the final light meson has a large (compared to its mass) recoil momentum (energy) in the rest frame of the decaying B meson almost in the whole kinematical range except the small region near the point of zero recoil. The maximum value of recoil momentum is of order of $m_b/2$. Thus near this point one can expand both in inverse powers of the heavy b quark mass and large recoil momentum of the final light meson. Such expansions lead to the so-called large-energy effective theory (LEET) [5], to a new symmetry, and as a result to the form factor relations in the heavy quark and large recoil limits [6,7]. Large values of the recoil momentum require the completely relativistic treatment of the semileptonic heavy-to-light B decays.

In our previous papers [8–10] we considered semileptonic B decays to heavy $D^{(*)}$ and light $\pi(\rho)$ mesons in the framework of the relativistic quark model based on the quasipotential approach. At that time taking into account large experimental errors in the measured decay rates we used the simple Gaussian parameterization for the meson wave functions. Moreover, we calculated the heavy-to-light decay form factors only at the point of maximum recoil of the final light meson using an expansion both in inverse powers of the heavy b quark and large recoil momentum of the light meson. Then we employed a Gaussian or pole parametrization of the form factors in order to extrapolate them to the whole kinematical range. Such substitutions and extrapolations induced significant theoretical errors in the obtained results, but the accuracy was sufficient compared to large experimental uncertainties. Since then, as it has been already mentioned before, the experimental accuracy improved significantly. The main aim of this paper is to revise our previous consider-

ations of semileptonic B decays substantially increasing the precision and reliability. This is achieved by using the wave functions of the heavy B, D and light π, ρ mesons which were obtained by calculating their mass spectra [11,12]. The complete expressions for the heavy-to-light decay form factors are used for calculations and the determination of their q^2 dependence, thus avoiding *ad hoc* parametrizations. In the following we concentrate on the study of the relativistic effects and, for simplicity, neglect short-distance radiative corrections [4] since their contribution does not exceed the uncertainty of our calculations.

The paper is organized as follows. In Sec. II we briefly describe our relativistic quark model. Then in Sec. III we discuss the relativistic calculation of the decay matrix element of the weak current between meson states in the quasipotential approach. Special attention is devoted to the contributions of the negative-energy states and the relativistic transformation of the wave functions from the rest to the moving reference frame. Semileptonic B decays to $D^{(*)}$ mesons are considered in Sec. IV using the heavy quark expansion in $1/m_Q$. Leading and subleading Isgur-Wise functions are explicitly determined as the overlap integrals of the initial and final meson wave functions. A comprehensive comparison with recent experimental data is given and on this basis the value of the CKM matrix element $|V_{cb}|$ is determined. In Sec. V semileptonic B decays to π and ρ are investigated. The parametrization of the calculated form factors in the whole kinematical range is given. Total and partial decay rates are compared with recent measurements and the value of the CKM matrix element $|V_{ub}|$ is extracted. Section VI contains our conclusions.

II. RELATIVISTIC QUARK MODEL

In the quasipotential approach a meson is described by the wave function of the bound quark-antiquark state, which satisfies the quasipotential equation [13] of the Schrödinger type [14]

$$\left(\frac{b^2(M)}{2\mu_R} - \frac{\mathbf{p}^2}{2\mu_R}\right)\Psi_M(\mathbf{p}) = \int \frac{d^3q}{(2\pi)^3} V(\mathbf{p}, \mathbf{q}; M)\Psi_M(\mathbf{q}),$$

(1)

where the relativistic reduced mass is

$$\mu_R = \frac{E_1 E_2}{E_1 + E_2} = \frac{M^4 - (m_1^2 - m_2^2)^2}{4M^3},$$

(2)

and E_1, E_2 are the center of mass energies on mass shell given by

$$E_1 = \frac{M^2 - m_2^2 + m_1^2}{2M}, \qquad E_2 = \frac{M^2 - m_1^2 + m_2^2}{2M}.$$

(3)

Here $M = E_1 + E_2$ is the meson mass, $m_{1,2}$ are the quark masses, and $\mathbf{p}$ is their relative momentum. In the center of mass system the relative momentum squared on mass shell reads

$$b^2(M) = \frac{[M^2 - (m_1 + m_2)^2][M^2 - (m_1 - m_2)^2]}{4M^2}. \quad (4)$$

The kernel $V(\mathbf{p}, \mathbf{q}; M)$ in Eq. (1) is the quasipotential operator of the quark-antiquark interaction. It is constructed with the help of the off-mass-shell scattering amplitude, projected onto the positive energy states. Constructing the quasipotential of the quark-antiquark interaction, we have assumed that the effective interaction is the sum of the usual one-gluon exchange term with the mixture of long-range vector and scalar linear confining potentials, where the vector confining potential contains the Pauli interaction. The quasipotential is then defined by [15]

$$V(\mathbf{p}, \mathbf{q}; M) = \bar{u}_1(p)\bar{u}_2(-p)\mathcal{V}(\mathbf{p}, \mathbf{q}; M)u_1(q)u_2(-q), \quad (5)$$

with

$$\mathcal{V}(\mathbf{p}, \mathbf{q}; M) = \tfrac{4}{3}\alpha_s D_{\mu\nu}(\mathbf{k})\gamma_1^\mu\gamma_2^\nu + V_{\text{conf}}^V(\mathbf{k})\Gamma_1^\mu\Gamma_{2;\mu}$$
$$+ V_{\text{conf}}^S(\mathbf{k}),$$

where α_s is the QCD coupling constant, $D_{\mu\nu}$ is the gluon propagator in the Coulomb gauge

$$D^{00}(\mathbf{k}) = -\frac{4\pi}{\mathbf{k}^2}, \qquad D^{ij}(\mathbf{k}) = -\frac{4\pi}{k^2}\left(\delta^{ij} - \frac{k^i k^j}{\mathbf{k}^2}\right),$$
$$D^{0i} = D^{i0} = 0, \quad (6)$$

and $\mathbf{k} = \mathbf{p} - \mathbf{q}$; γ_μ and $u(p)$ are the Dirac matrices and spinors

$$u^\lambda(p) = \sqrt{\frac{\epsilon(p) + m}{2\epsilon(p)}}\begin{pmatrix} 1 \\ \frac{\boldsymbol{\sigma}\mathbf{p}}{\epsilon(p)+m} \end{pmatrix}\chi^\lambda. \quad (7)$$

Here $\boldsymbol{\sigma}$ and χ^λ are the Pauli matrices and spinors; $\epsilon(p) = \sqrt{p^2 + m^2}$. The effective long-range vector vertex is given by

$$\Gamma_\mu(\mathbf{k}) = \gamma_\mu + \frac{i\kappa}{2m}\sigma_{\mu\nu}k^\nu, \quad (8)$$

where κ is the Pauli interaction constant characterizing the long-range anomalous chromomagnetic moment of quarks. Vector and scalar confining potentials in the nonrelativistic limit reduce to

$$V_V(r) = (1 - \varepsilon)(Ar + B), \qquad V_S(r) = \varepsilon(Ar + B), \quad (9)$$

reproducing

$$V_{\text{conf}}(r) = V_S(r) + V_V(r) = Ar + B, \quad (10)$$

where ε is the mixing coefficient.

The expression for the quasipotential of the heavy quarkonia, expanded in v^2/c^2 without and with retardation corrections to the confining potential, can be found in Refs. [15,16], respectively. The structure of the spin-dependent interaction is in agreement with the parametrization of Eichten and Feinberg [17]. The quasipotential for the heavy quark interaction with a light antiquark without employing the nonrelativistic (v/c) expansion for the light quark is given in Ref. [11]. All the parameters of our model like quark masses, parameters of the linear confining potential A and B, mixing coefficient ε, and anomalous chromomagnetic quark moment κ are fixed from the analysis of heavy quarkonium masses [15] and radiative decays [18]. The quark masses $m_b = 4.88$ GeV, $m_c = 1.55$ GeV, $m_{u,d} = 0.33$ GeV and the parameters of the linear potential $A = 0.18$ GeV^2 and $B = -0.30$ GeV have usual values of quark models. The value of the mixing coefficient of vector and scalar confining potentials $\varepsilon = -1$ has been determined from the consideration of the heavy quark expansion for the semileptonic $B \to D$ decays [8] and charmonium radiative decays [18]. Finally, the universal Pauli interaction constant $\kappa = -1$ has been fixed from the analysis of the fine splitting of heavy quarkonia ^3P_J- states [15]. Note that the long-range magnetic contribution to the potential in our model is proportional to $(1 + \kappa)$ and thus vanishes for the chosen value of $\kappa = -1$. It has been known for a long time that the correct reproduction of the spin-dependent part of the quark-antiquark interaction requires either assuming the scalar confinement or equivalently introducing the Pauli interaction with $\kappa = -1$ [15,16,19] in the vector confinement.

III. MATRIX ELEMENTS OF THE WEAK CURRENT FOR $b \to c, u$ TRANSITIONS

In order to calculate the exclusive semileptonic decay rate of the B meson, it is necessary to determine the corresponding matrix element of the weak current between meson states. In the quasipotential approach, the matrix element of the weak current $J_\mu^W = \bar{f}\gamma_\mu(1 - \gamma_5)b$, associated with $b \to f$ ($f = c$ or u) transition, between a B meson with mass M_B and momentum p_B and a final meson F ($F = D^{(*)}$ or $\pi(\rho)$) with mass M_F and momentum p_F takes the form [20]

$$\langle F(p_F)|J_\mu^W|B(p_B)\rangle = \int \frac{d^3p\, d^3q}{(2\pi)^6} \bar{\Psi}_{F\mathbf{p}_F}(\mathbf{p})\Gamma_\mu(\mathbf{p}, \mathbf{q})\Psi_{B\mathbf{p}_B}(\mathbf{q}),$$
$$(11)$$

where $\Gamma_\mu(\mathbf{p}, \mathbf{q})$ is the two-particle vertex function and $\Psi_{M\mathbf{p}_M}$ are the meson ($M = B, F$) wave functions projected onto the positive energy states of quarks and boosted to the moving reference frame with momentum $\mathbf{p}_M$.

The contributions to Γ come from Figs. 1 and 2. The leading order vertex function $\Gamma^{(1)}$ corresponds to the impulse approximation, while the vertex function $\Gamma^{(2)}$ accounts for contributions of the negative-energy states. Note that the form of the relativistic corrections resulting from the vertex function $\Gamma^{(2)}$ is explicitly dependent on the Lorentz structure of the quark-antiquark interaction. In the leading order of the heavy quark expansion ($m_{b,c} \to \infty$) for $B \to D$ transitions only $\Gamma^{(1)}$ contributes, while $\Gamma^{(2)}$ con-
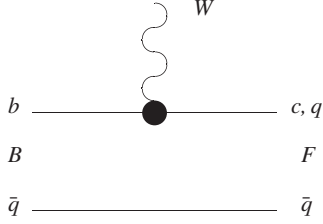
FIG. 1.   Lowest order vertex function $\Gamma^{(1)}$ contributing to the current matrix element (11).

tributes already at the subleading order. The vertex functions look like

$$\Gamma_\mu^{(1)}(\mathbf{p}, \mathbf{q}) = \bar{u}_f(p_f)\gamma_\mu(1 - \gamma^5)u_b(q_b)(2\pi)^3\delta(\mathbf{p}_q - \mathbf{q}_q), \tag{12}$$

and

$$\begin{aligned}\Gamma_\mu^{(2)}(\mathbf{p}, \mathbf{q}) = \bar{u}_f(p_f)\bar{u}_q(p_q)\Big\{&\gamma_{1\mu}(1 - \gamma_1^5)\frac{\Lambda_b^{(-)}(k)}{\epsilon_b(k) + \epsilon_b(p_q)}\\ &\times \gamma_1^0\mathcal{V}(\mathbf{p}_q - \mathbf{q}_q) + \mathcal{V}(\mathbf{p}_q - \mathbf{q}_q)\\ &\times \frac{\Lambda_f^{(-)}(k')}{\epsilon_f(k') + \epsilon_f(q_f)}\gamma_1^0\gamma_{1\mu}(1 - \gamma_1^5)\Big\}u_b(q_b)u_q(q_q),\end{aligned} \tag{13}$$

where the superscripts "(1)" and "(2)" correspond to Figs. 1 and 2, $\mathbf{k} = \mathbf{p}_f - \boldsymbol{\Delta}$; $\mathbf{k}' = \mathbf{q}_b + \boldsymbol{\Delta}$; $\boldsymbol{\Delta} = \mathbf{p}_F - \mathbf{p}_B$;

$$\Lambda^{(-)}(p) = \frac{\epsilon(p) - (m\gamma^0 + \gamma^0(\boldsymbol{\gamma}\mathbf{p}))}{2\epsilon(p)}.$$

Here [20]

$$p_{f,q} = \epsilon_{f,q}(p)\frac{p_F}{M_F} \pm \sum_{i=1}^3 n^{(i)}(p_F)p^i,$$

$$q_{b,q} = \epsilon_{b,q}(q)\frac{p_B}{M_B} \pm \sum_{i=1}^3 n^{(i)}(p_B)q^i,$$

and $n^{(i)}$ are three four-vectors given by

$$n^{(i)\mu}(p) = \left\{\frac{p^i}{M}, \delta_{ij} + \frac{p^ip^j}{M(E + M)}\right\}, \qquad E = \sqrt{\mathbf{p}^2 + M^2}.$$
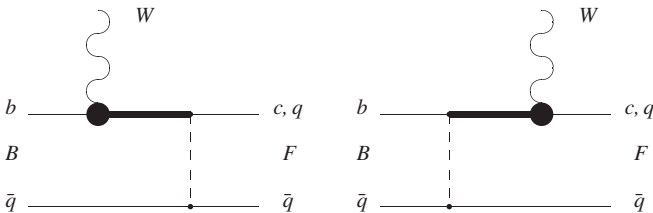
FIG. 2.   Vertex function $\Gamma^{(2)}$ taking the quark interaction into account. Dashed lines correspond to the effective potential $\mathcal{V}$ in (5). Bold lines denote the negative-energy part of the quark propagator.

It is important to note that the wave functions entering the weak current matrix element (11) are not in the rest frame in general. For example, in the B meson rest frame ($\mathbf{p}_B = 0$), the final meson is moving with the recoil momentum $\boldsymbol{\Delta}$. The wave function of the moving meson $\Psi_{F\boldsymbol{\Delta}}$ is connected with the wave function in the rest frame $\Psi_{F0} \equiv \Psi_F$ by the transformation [20]

$$\Psi_{F\boldsymbol{\Delta}}(\mathbf{p}) = D_f^{1/2}(R_{L_{\boldsymbol{\Delta}}}^W)D_q^{1/2}(R_{L_{\boldsymbol{\Delta}}}^W)\Psi_{F0}(\mathbf{p}), \tag{14}$$

where R^W is the Wigner rotation, $L_{\boldsymbol{\Delta}}$ is the Lorentz boost from the meson rest frame to a moving one, and the rotation matrix $D^{1/2}(R)$ in spinor representation is given by

$$\begin{pmatrix} 1 & 0 \\ 0 & 1 \end{pmatrix}D_{q,c}^{1/2}(R_{L_{\boldsymbol{\Delta}}}^W) = S^{-1}(\mathbf{p}_{q,c})S(\boldsymbol{\Delta})S(\mathbf{p}), \tag{15}$$

where

$$S(\mathbf{p}) = \sqrt{\frac{\epsilon(p) + m}{2m}}\left(1 + \frac{\boldsymbol{\alpha}\mathbf{p}}{\epsilon(p) + m}\right)$$

is the usual Lorentz transformation matrix of the four-spinor.

The general structure of the current matrix element (11) is rather complicated, because it is necessary to integrate both with respect to d^3p and d^3q. The δ-function in the expression (12) for the vertex function $\Gamma^{(1)}$ permits to perform one of these integrations. As a result the contribution of $\Gamma^{(1)}$ to the current matrix element has the usual structure of an overlap integral of meson wave functions and can be calculated exactly (without employing any expansion) in the whole kinematical range, if the wave functions of the initial and final mesons are known. The situation with the contribution $\Gamma^{(2)}$ is different. Here, instead of a δ-function, we have a complicated structure, containing the potential of the $q\bar{q}$-interaction in the meson. It contains also the quark energies $\epsilon_q(p) = \sqrt{m_q^2 + \mathbf{p}^2}$, which explicitly depend on the relative quark momentum $\mathbf{p}$. The presence of such dependence does not permit one, in the general case, to get rid of one of the integrations in the contribution of $\Gamma^{(2)}$ to the matrix element (11). Therefore, it is necessary to use some additional considerations in order to simplify calculations. The main idea is to expand the vertex function $\Gamma^{(2)}$, given by (13), in such a way that it will be possible to use the quasipotential Eq. (1) in order to perform one of the integrations in the current matrix element (11) and thus express this contribution to the decay matrix element through the usual overlap integral of meson wave functions. The realization of this strategy differs for the cases of heavy-to-heavy and heavy-to-light transitions.

IV. SEMILEPTONIC B MESON DECAYS TO D MESONS

For the description of semileptonic B decays to ground state D mesons (heavy-to-heavy transitions) it is conve-

nient to use the HQET parametrization for the decay matrix elements [4]:

$$\frac{\langle D(v')|\bar{c}\gamma^\mu b|B(v)\rangle}{\sqrt{M_D M_B}} = h_+(v+v')^\mu + h_-(v-v')^\mu,$$

$$\langle D(v')|\bar{c}\gamma^\mu b\gamma_5|B(v)\rangle = 0,$$

$$\frac{\langle D^*(v',\epsilon)|\bar{c}\gamma^\mu b|B(v)\rangle}{\sqrt{M_{D^*} M_B}} = ih_V \varepsilon^{\mu\alpha\beta\gamma}\epsilon^*_\alpha v'_\beta v_\gamma, \qquad (16)$$

$$\frac{\langle D^*(v',\epsilon)|\bar{c}\gamma^\mu \gamma_5 b|B(v)\rangle}{\sqrt{M_{D^*} M_B}} = h_{A_1}(w+1)\epsilon^{*\mu}$$
$$- (h_{A_2}v^\mu + h_{A_3}v'^\mu)(\epsilon^* \cdot v),$$

where $v(v')$ is the four-velocity of the $B(D^{(*)})$ meson, ϵ^μ is the polarization vector of the final vector meson, and the form factors h_i are dimensionless functions of the product of four-velocities

$$w = v \cdot v' = \frac{M_B^2 + M_{D^{(*)}}^2 - q^2}{2M_B M_{D^{(*)}}},$$

and $q = p_B - p_{D^{(*)}}$ is the momentum transfer from the parent to daughter meson.

In HQET these form factors up to $1/m_Q$ are given by [4]

$$h_+ = \xi + (\varepsilon_c + \varepsilon_b)[2\chi_1 - 4(w-1)\chi_2 + 12\chi_3], \qquad h_- = (\varepsilon_c - \varepsilon_b)[2\xi_3 - \bar{\Lambda}\xi],$$

$$h_V = \xi + \varepsilon_c[2\chi_1 - 4\chi_3 + \bar{\Lambda}\xi] + \varepsilon_b[2\chi_1 - 4(w-1)\chi_2 + 12\chi_3 + \bar{\Lambda}\xi - 2\xi_3],$$

$$h_{A_1} = \xi + \varepsilon_c\left[2\chi_1 - 4\chi_3 + \frac{w-1}{w+1}\bar{\Lambda}\xi\right] + \varepsilon_b\left[2\chi_1 - 4(w-1)\chi_2 + 12\chi_3 + \frac{w-1}{w+1}(\bar{\Lambda}\xi - 2\xi_3)\right], \qquad (17)$$

$$h_{A_2} = \varepsilon_c\left[4\chi_2 - \frac{2}{w+1}(\bar{\Lambda}\xi + \xi_3)\right],$$

$$h_{A_3} = \xi + \varepsilon_c\left[2\chi_1 - 4\chi_2 - 4\chi_3 + \frac{w-1}{w+1}\bar{\Lambda}\xi^{(n)} - \frac{2}{w+1}\xi_3\right] + \varepsilon_b[2\chi_1 - 4(w-1)\chi_2 + 12\chi_3 + \bar{\Lambda}\xi - 2\xi_3].$$

The calculation of the weak transition $B \rightarrow D^{(*)}$ matrix elements using the heavy quark expansion shows that all model independent HQET relations are satisfied in our model. In the limit of an infinitely heavy quark all form factors are expressed through the Isgur-Wise function [2]

$$h_+(w) = h_{A_1}(w) = h_{A_3}(w) = h_V(w) = \xi(w),$$
$$h_-(w) = h_{A_2}(w) = 0. \qquad (18)$$

In our model this function is given as the overlap integral of meson wave functions [8]

$$\xi(w) = \sqrt{\frac{2}{w+1}}\lim_{m_Q\to\infty}\int \frac{d^3p}{(2\pi)^3}\bar{\Psi}_D\left(\mathbf{p} + 2\epsilon_q(p)\right.$$
$$\left.\times \sqrt{\frac{w-1}{w+1}}\mathbf{e_\Delta}\right)\Psi_B(\mathbf{p}), \qquad (19)$$

where $\mathbf{e_\Delta} = \mathbf{\Delta}/\sqrt{\mathbf{\Delta}^2}$ is the unit vector in the direction of $\mathbf{\Delta} = M_D\mathbf{v}' - M_B\mathbf{v}$. In order to fulfill the HQET relations (17) in the first order of the heavy quark $1/m_Q$ expansion it is necessary to set $(1-\varepsilon)(1+\kappa) = 0$, which leads to the vanishing long-range chromomagnetic interaction. This condition is satisfied by our choice of the anomalous chromomagnetic quark moment $\kappa = -1$. To fulfill the HQET relations at second order in $1/m_Q$ it is necessary to set $\varepsilon = -1$ [8]. This gives an additional justification, based on the heavy quark symmetry and heavy quark expansion in QCD, of the choice of the characteristic parameters of our model. In the infinitely heavy quark mass limit the wave functions of initial Ψ_B and final Ψ_D

heavy mesons coincide. As the result the HQET normalization condition [4]

$$\xi(1) = 1$$

is exactly reproduced. The first order Isgur-Wise functions are given by [8]

$$\xi_3(w) = (\bar{\Lambda} - m_q)\left(1 + \frac{2}{3}\frac{w-1}{w+1}\right)\xi(w),$$

$$\chi_1(w) = \bar{\Lambda}\frac{w-1}{w+1}\xi(w),$$

$$\chi_2(w) = -\frac{1}{32}\frac{\bar{\Lambda}}{w+1}\xi(w), \qquad (20)$$

$$\chi_3(w) = \frac{1}{16}\bar{\Lambda}\frac{w-1}{w+1}\xi(w),$$

where the HQET parameter $\bar{\Lambda} = M - m_Q$ is equal to the mean energy of a light quark in a heavy meson

$$\bar{\Lambda} = \langle\varepsilon_q\rangle \simeq 0.56 \text{ GeV}.$$

The functions χ_1 and χ_3 explicitly satisfy normalization conditions at the zero recoil point [21]

$$\chi_1(1) = \chi_3(1) = 0,$$

arising from vector current conservation.

In Figs. 3–5 we plot the Isgur-Wise functions calculated with numerical wave functions determined in the process of their mass calculations [11]. Near the zero recoil point of the final meson $w = 1$ the Isgur-Wise function can be written as
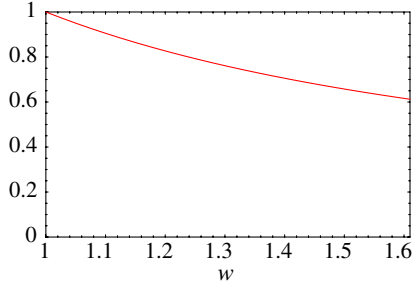
FIG. 3 (color online).   The Isgur-Wise function $\xi(w)$.

$$\xi(w) = 1 - \rho^2(w - 1) + c(w - 1)^2 + \cdots, \qquad (21)$$

where $\rho^2 = -[d\xi(w)/dw]_{w=1} \simeq 1.04$ is the slope and $c = (1/2)[d^2\xi(w)/d^2w]_{w=1} \simeq 1.36$ is the curvature of the Isgur-Wise function. The slope ρ^2 can be compared to the recent quenched lattice QCD evaluation [22]: $\rho^2 = 0.83^{+15+24}_{-11-22}$. Note that both the slope and curvature of the calculated Isgur-Wise function satisfy all known lower bounds (see Ref. [23] and references therein).

The differential semileptonic decay rate $B \to Dl\bar{\nu}$ for the massless leptons is given by [4]

$$\frac{d\Gamma}{dw} = \frac{G_F^2}{48\pi^3}|V_{cb}|^2 M_D^3(w^2 - 1)^{3/2}(M_B + M_D)^2 F_D^2(w),$$
$$(22)$$

where G_F is the Fermi constant, and the form factor $F_D(w)$ is defined by

$$F_D(w) = \left[h_+(w) - \frac{1 - r}{1 + r}h_-(w)\right], \qquad r = \frac{M_D}{M_B}. \quad (23)$$

Near the zero recoil point the form factor $F_D(w)$ has the following expansion

$$F_D(w) = F_D(1)[1 - \rho_D(w - 1) + c_D(w - 1)^2 + \cdots],$$
$$(24)$$

where the value of $F_D(1)$, calculated by using the unexpanded in $1/m_Q$ expressions (A1)–(A3) of Ref. [9], is equal to

$$F_D(1) = 0.966. \qquad (25)$$
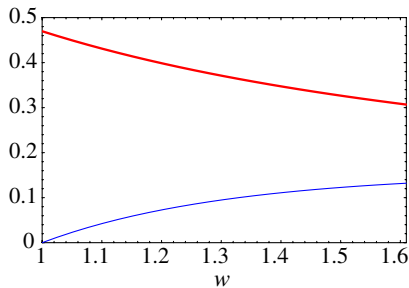
FIG. 4 (color online).   The first order functions $\xi_3(w)/\bar{\Lambda}$ (bold line) and $\chi_1(w)/\bar{\Lambda}$ (solid line).
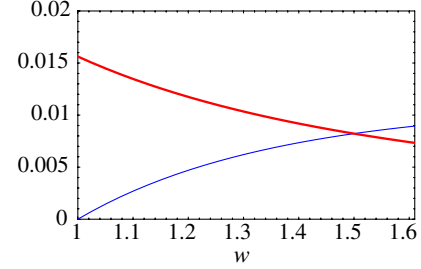
FIG. 5 (color online).   The first order functions $-\chi_2(w)/\bar{\Lambda}$ (bold line) and $\chi_3(w)/\bar{\Lambda}$ (solid line).

Quenched lattice QCD calculations [24] give the value $F_D(1) = 1.058 \pm 0.016 \pm 0.03^{+0.014}_{-0.005}$, while Ref. [25] predicts $F_D(1) = 0.98 \pm 0.07$.

The slope of the form factor $F_D(w)$ at zero recoil $w = 1$ in our model

$$\rho_D^2 = -\frac{1}{F_D(w)} \frac{dF_D(w)}{dw} \bigg|_{w=1} = 0.88, \qquad (26)$$

is in good agreement with experimental values $\rho_D^2 = 0.76 \pm 0.16 \pm 0.08$ [26] and $\rho_D^2 = 0.69 \pm 0.14$ [27], obtained by using the linear fit of the data. The curvature of the form factor $F_D(w)$ is equal to $c_D = [1/(2F_D(1))] \times [d^2F_D(w)/d^2w]_{w=1} \simeq 0.75$.

In Fig. 6 we compare the results of our model for the product $F_D(w)|V_{cb}|$ with the recent experimental data of CLEO [26] and Belle [27]. It is seen that the form factor $F_D(w)$ dependence on w in our model is in good agreement with measurements. The combined fit of CLEO ($F_D(1)|V_{cb}| = 0.039 \pm 0.002$) and Belle ($F_D(1)|V_{cb}| = 0.041 \pm 0.003$) data leads to the value of the product of the form factor and CKM matrix element

$$F_D(1)|V_{cb}| = 0.040 \pm 0.002.$$
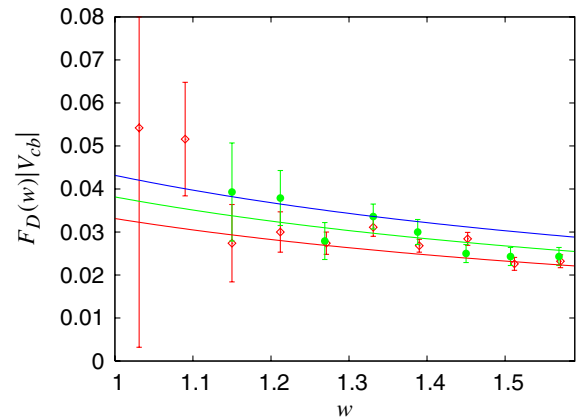
FIG. 6 (color online).   Comparison of experimental data and predictions of our model for the product $F_D(w)|V_{cb}|$. Dots represent CLEO data [26] and diamonds show Belle data [27]. Solid lines are predictions of our model for $|V_{cb}| = 0.044, 0.039, 0.034$ (from top to bottom, respectively).

Using our prediction (25) for the form factor $F_D(1)$ we find the value of CKM matrix element

$$|V_{cb}| = 0.0415 \pm 0.0020. \qquad (27)$$

The differential semileptonic decay rate $B \to D^* l\bar{\nu}$ is defined by [4]

$$\frac{d\Gamma}{dw} = \frac{G_F^2}{48\pi^3} |V_{cb}|^2 (M_B - M_{D^*})^2 M_{D^*}^3 \sqrt{(w^2 - 1)}(w + 1)^2$$

$$\times \left[1 + \frac{4w}{w+1} \frac{1 - 2wr^* + r^{*2}}{(1 - r^*)^2} \right] F_{D^*}^2(w),$$

$$r^* = \frac{M_{D^*}}{M_B}, \qquad (28)$$

where the form factor $F_{D^*}(w)$ is given by

$$F_{D^*}(w) = h_{A_1}(w) \sqrt{\frac{\tilde{H}_+^2(w) + \tilde{H}_-^2(w) + \tilde{H}_0^2(w)}{1 + \frac{4w}{w+1} \frac{1 - 2wr^* + r^{*2}}{(1 - r^*)^2}}}. \qquad (29)$$

The helicity amplitudes $\tilde{H}_j(w)$

$$\tilde{H}_\pm(w) = \frac{\sqrt{1 - 2wr^* + r^{*2}}}{1 - r^*} \left[1 \mp \sqrt{\frac{w-1}{w+1}} R_1(w) \right],$$

$$\tilde{H}_0(w) = 1 + \frac{w-1}{1-r^*}[1 - R_2(w)]r \qquad (30)$$

are expressed through form factor ratios

$$R_1(w) = \frac{h_V(w)}{h_{A_1}(w)}, \qquad R_2(w) = \frac{h_{A_3}(w) + r^* h_{A_2}(w)}{h_{A_1}(w)}. \qquad (31)$$

In the limit $m_Q \to \infty$, $R_1 = R_2 = 1$ due to spin-flavor symmetry [4]. Taking into account of $1/m_Q$ corrections breaks down this symmetry relation. In our model using unexpanded in $1/m_Q$ formulas for the form factors [9] we get the following expressions near the zero recoil point $w = 1$

$$h_{A_1}(w) = 0.918[1 - 0.86(w - 1) + 0.72(w - 1)^2 + \cdots],$$

$$F_{D^*}(w) = 0.918[1 - 0.66(w - 1) + 0.17(w - 1)^2 + \cdots],$$

$$R_1(w) = 1.39 - 0.23(w - 1) + 0.21(w - 1)^2 + \cdots,$$

$$R_2(w) = 0.92 + 0.12(w - 1) - 0.07(w - 1)^2 + \cdots. \qquad (32)$$

It is necessary to note that the behavior of the form factor $h_{A_1}(w)$ predicted by our model agrees, in general, with the parametrization [28] in the whole kinematical range. On the other hand, the expansion of the form factor ratios R_1 and R_2 is close to the QCD sum rule results [4]. Lattice QCD calculation [29] gives the value of $h_{A_1}(1) = 0.9130^{+0.0238+0.0171}_{-0.0173-0.0302}$. Our result for the difference of the slope parameters

$$\rho_{A_1}^2 - \rho_{D^*}^2 = 0.20$$

is in agreement with previous calculations 0.21 [25] and 0.17 [30]. Comparing Eqs. (26) and (32) we find the value of the slope difference

$$\rho_{A_1}^2 - \rho_D^2 = -0.02,$$

which coincides with the one found in Ref. [30].

In Table I we give our predictions for $R_1(1)$, $R_2(1)$ and for the slope of the form factor h_{A_1} and available experimental data [31–34]. Our results for R_1 and R_2 agree well with the data. The calculated slope $\rho_{h_{A_1}}^2$ is within experimental error bars for the values obtained by using a linear fit. Comparison of our predictions for the product $F_{D^*}(w)|V_{cb}|$ with the experimental data from CLEO [31], Belle [33], and *BABAR* [32] is given in Fig. 7. In general there is good agreement between the calculated form factor behavior and available experimental data. The values of the product $F_{D^*}(1)|V_{cb}|$, obtained by using our form factors are compared in Table I with the ones based on the parametrization of the form factor h_{A_1} from Ref. [28]. Our model leads to the values of the product $F_{D^*}(1)|V_{cb}|$ approximately 10%–15% lower than the values obtained using the parametrization [28]. A combined fit of all above mentioned experimental data in the framework of our model gives

TABLE I. Comparison of our model predictions for the ratios $R_1(1)$, $R_2(1)$, the slope of the form factor h_{A_1} for $w = 1$, and values of the product $F_{D^*}(1)|V_{cb}|$ with experimental data.

	Our	CLEO [31]	*BABAR* [32]	Belle [33]	DELPHI [34]
R_1	1.39	1.18(30)(12)	1.396(60)(44)		
R_2	0.92	0.71(22)(7)	0.885(40)(26)		
$\rho_{h_{A_1}}^2$	0.86	0.91(15)(6)[a] 1.61(9)(21)[b]	0.79(6)[a] 1.145(59)(46)[b]	0.81(12)[a] 1.35(17)[b]	1.39(10)(33)[b]
$F_{D^*}|V_{cb}|$	0.0343(12)	0.0360(20)[c] 0.0431(13)(18)[b]	0.0328(5)[c] 0.0376(3)(16)[b]	0.0315(12)[c] 0.0354(19)(18)[b]	0.0377(11)(19)[b]

[a]Linear fit of experimental data.
[b]Fit using the form factor h_{A_1} parametrization [28].
[c]Fit using form factor predictions of our model.
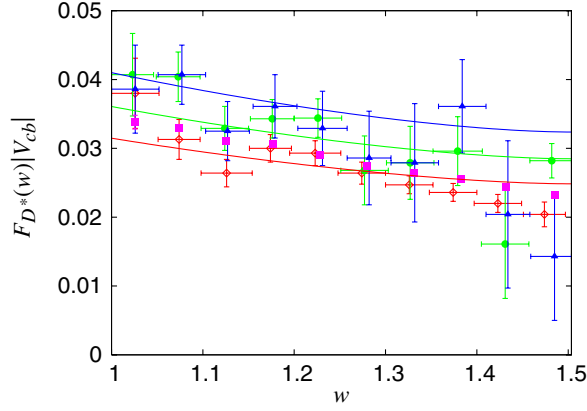
FIG. 7 (color online). Comparison of experimental data and predictions of our model for the product $F_{D^*}(w)|V_{cb}|$. Dots show CLEO data for $B^+ \to D^{*0}l^-\nu$, triangles—CLEO data for $B^0 \to D^{*+}l^-\nu$ [31], diamonds—Belle data [33], squares—BABAR data [32]. Solid lines show predictions of our model for $|V_{cb}| = 0.044, 0.039, 0.034$ (from top to bottom, respectively).

$$F_{D^*}(1)|V_{cb}| = 0.0343 \pm 0.012.$$

Using our value of $F_{D^*}(1) = h_{A_1}(1) = 0.918$ (see (32)) we get

$$|V_{cb}| = 0.0375 \pm 0.0015. \tag{33}$$

The theoretical results for the ratios $R_1(1)$, $R_2(1)$ and their derivatives $R_1'(1)$, $R_2'(1)$ are confronted in Table II. In general there is a reasonable agreement both for the form factor ratios and their slopes. Our values are very close to the ones found using HQET and QCD sum rules [4].

By integrating the expressions for the differential decay rates (22) and (28), we get predictions for the total decay rates in our model

$$\Gamma(B \to Dl\nu) = 9.48|V_{cb}|^2 \text{ ps}^{-1},$$
$$\Gamma(B \to D^*l\nu) = 24.9|V_{cb}|^2 \text{ ps}^{-1}. \tag{34}$$

Taking mean values of lifetimes [37]: $\tau_{B^0} = 1.530 \times 10^{-12}$ s and $\tau_{B^+} = 1.671 \times 10^{-12}$ s, we find

TABLE II. Comparison of theoretical predictions for the ratios $R_1(1)$, $R_2(1)$, and their derivatives $R_1'(1)$, $R_2'(1)$.

Ref.	$R_1(1)$	$R_1'(1)$	$R_2(1)$	$R_2'(1)$
Our	1.39	-0.23	0.92	0.12
[30]	1.25	-0.10	0.81	0.11
[25]	1.27	-0.12	0.80	0.11
[4]	1.35	-0.22	0.79	0.15
[35]	1.15		0.94	
[36]	1.01(2)		1.04(1)	

$$\text{BR}(B^0 \to D^+l^-\nu) = 14.5|V_{cb}|^2,$$
$$\text{BR}(B^+ \to D^0l^+\nu) = 15.8|V_{cb}|^2,$$
$$\text{BR}(B^0 \to D^{*+}l^-\nu) = 38.0|V_{cb}|^2,$$
$$\text{BR}(B^+ \to D^{*0}l^+\nu) = 41.3|V_{cb}|^2. \tag{35}$$

The comparison of theoretical and experimental branching ratios [37] leads to the following values of the CKM matrix element $|V_{cb}|$:

$$\text{BR}(B^0 \to D^+l^-\nu)^{\text{exp}} = 0.0214 \pm 0.0020$$
$$|V_{cb}| = 0.038 \pm 0.002,$$
$$\text{BR}(B^+ \to D^0l^+\nu)^{\text{exp}} = 0.0215 \pm 0.0022$$
$$|V_{cb}| = 0.037 \pm 0.002,$$
$$\text{BR}(B^0 \to D^{*+}l^-\nu)^{\text{exp}} = 0.0544 \pm 0.0023$$
$$|V_{cb}| = 0.038 \pm 0.001,$$
$$\text{BR}(B^+ \to D^{*0}l^+\nu)^{\text{exp}} = 0.065 \pm 0.005$$
$$|V_{cb}| = 0.040 \pm 0.002, \tag{36}$$

which are in good agreement with each other and with values (27) and (33), found from the form factor analysis. Thus the averaged $|V_{cb}|$ over all presented experimental measurements of semileptonic decays $B \to De\nu$ and $B \to D^*e\nu$ is equal to

$$|V_{cb}| = 0.0385 \pm 0.0015 \tag{37}$$

in good agreement with PDG [37]

$$|V_{cb}| = 0.0409 \pm 0.0018 \qquad \text{(exclusive)}.$$

V. SEMILEPTONIC *B* DECAYS TO LIGHT MESONS

The matrix elements of weak current J^W governing the weak *B* decays to the light pseudoscalar meson ($P = \pi$) is parametrized by two invariant form factors. It is convenient to use the following decomposition:

$$\langle P(p_F)|\bar{q}\gamma^\mu b|B(p_B)\rangle = f_+(q^2)\left[p_B^\mu + p_F^\mu - \frac{M_B^2 - M_P^2}{q^2}q^\mu \right]$$
$$+ f_0(q^2)\frac{M_B^2 - M_P^2}{q^2}q^\mu, \tag{38}$$

where $q = p_B - p_F$; M_B is the *B* meson and M_P is the final pseudoscalar meson mass.

The corresponding matrix elements for the weak *B* decays to the light vector meson ($V = \rho$) can be parametrized by four form factors:

$$\langle V(p_F)|\bar{q}\gamma^\mu b|B(p_B)\rangle = \frac{2iV(q^2)}{M_B + M_V} \epsilon^{\mu\nu\rho\sigma} \epsilon_\nu^* p_{B\rho} p_{F\sigma}, \tag{39}$$

$$\langle V(p_F)|\bar{q}\gamma^\mu\gamma_5 b|B(p_B)\rangle = 2M_V A_0(q^2)\frac{\epsilon^* \cdot q}{q^2}q^\mu$$
$$+ (M_B + M_V)A_1(q^2)$$
$$\times \left(\epsilon^{*\mu} - \frac{\epsilon^* \cdot q}{q^2}q^\mu\right)$$
$$- A_2(q^2)\frac{\epsilon^* \cdot q}{M_B + M_V}$$
$$\times \left[p_B^\mu + p_F^\mu - \frac{M_B^2 - M_V^2}{q^2}q^\mu\right],$$
$$(40)$$

where M_V and ϵ_μ are the mass and polarization vector of the final vector meson. At the maximum recoil point ($q^2 = 0$) these form factors satisfy the relations:

$$f_+(0) = f_0(0),$$
$$A_0(0) = \frac{M_B + M_V}{2M_V}A_1(0) - \frac{M_B - M_V}{2M_V}A_2(0).$$

For massless leptons form factors f_0 and A_0 do not contribute to the semileptonic decay rates. However they give contributions to the nonleptonic decay rates in the factorization approximation. Note that this parametrization is completely equivalent to the one of HQET (16), and corresponding form factors can be easily expressed through each other.

In this section we calculate semileptonic decay rates of the heavy *B* meson into light meson, $B \to \pi(\rho)e\nu$. The final meson in these decays contains light quarks (u, d, s) only, thus in contrast to decays to heavy *D* mesons, considered previously, the application of the expansion in inverse powers of the final active quark is not justified. The calculation of the contribution of the vertex function $\Gamma^{(1)}$ (12) to the decay matrix element of the weak current (11) can, as it was already in detail discussed above, be carried out exactly, due to the presence of δ-function, and does not require any expansion. The calculation of the contribution $\Gamma^{(2)}$ is significantly more difficult, since the expansion only in inverse powers of the heavy *b*-quark mass from the initial *B* meson retains the dependence on the relative momentum in the energy of the final light quark. Such dependence does not allow one to perform one of the integrals in the decay matrix element (11) using the quasipotential equation. However the final light meson has a large (compared to its mass) recoil momentum ($\Delta \equiv \mathbf{p}_F - \mathbf{p}_B$, $|\Delta_{max}| = (M_B^2 - M_F^2)/(2M_B) \cong M_B/2 \sim 2.6$ GeV) almost in the whole kinematical range except the small region near $q^2 = q_{max}^2$ ($|\Delta| = 0$). This also means that the recoil momentum of the final meson is large with respect to the mean relative quark momentum $|\mathbf{p}|$ in the meson (~ 0.5 GeV). Thus one can neglect $|\mathbf{p}|$ compared to $|\Delta|$ in the final light quark energy $\epsilon_q(p + \Delta) \equiv \sqrt{m_q^2 + (\mathbf{p} + \Delta)^2}$, replacing it by $\epsilon_q(\Delta) \equiv \sqrt{m_q^2 + \Delta^2}$ in

expressions for the $\Gamma^{(2)}$ contribution in accord with the large-energy expansion (see Introduction). This replacement removes the relative momentum dependence in the energy of the light quark and thus permits to perform one of the integrations in the $\Gamma^{(2)}$ contribution using the quasipotential equation. Note that the relatively small value of this contribution, related to its proportionality to the binding energy in the meson, and its predictable momentum dependence allow us to extrapolate it to the whole kinematical range. The numerical analysis (see below) shows that such extrapolation induces insignificant uncertainties in the final results for decay rates.

It is convenient to consider semileptonic decays $B \to (\pi, \rho)e\nu$ in the *B* meson rest frame. Then calculating decay matrix elements it is necessary to take into account the relativistic transformation (14) of the final meson wave function from the rest frame to the moving one with the momentum Δ. Applying the method described above, we find expressions for the decay matrix element and determine the corresponding form factors. They have the following structure:

(a) $B \to \pi$ transitions

$$f_+(q^2) = f_+^{(1)}(q^2) + \varepsilon f_+^{S(2)}(q^2) + (1 - \varepsilon)f_+^{V(2)}(q^2),$$
$$(41)$$

$$f_0(q^2) = f_0^{(1)}(q^2) + \varepsilon f_0^{S(2)}(q^2) + (1 - \varepsilon)f_0^{V(2)}(q^2),$$
$$(42)$$

(b) $B \to \rho$ transitions

$$V(q^2) = V^{(1)}(q^2) + \varepsilon V^{S(2)}(q^2) + (1 - \varepsilon)V^{V(2)}(q^2),$$
$$(43)$$

$$A_1(q^2) = A_1^{(1)}(q^2) + \varepsilon A_1^{S(2)}(q^2) + (1 - \varepsilon)A_1^{V(2)}(q^2),$$
$$(44)$$

$$A_2(q^2) = A_2^{(1)}(q^2) + \varepsilon A_2^{S(2)}(q^2) + (1 - \varepsilon)A_2^{V(2)}(q^2),$$
$$(45)$$

$$A_0(q^2) = A_0^{(1)}(q^2) + \varepsilon A_0^{S(2)}(q^2) + (1 - \varepsilon)A_0^{V(2)}(q^2),$$
$$(46)$$

where expressions for $f_{+,0}^{(1)}$, $f_{+,0}^{S,V(2)}$, $A_{0,1,2}^{(1)}$, $A_{0,1,2}^{S,V(2)}$, $V^{(1)}$, and $V^{S,V(2)}$ are rather cumbersome and can be found in the appendix to Ref. [10]. The subscripts "(1)" and "(2)" correspond to Figs. 1 and 2, *S* and *V* denote scalar and vector potentials of the $q\bar{q}$-interaction. Let us remind that the mixing coefficient ε of vector and scalar confining potentials is equal to -1 in our model. Note that form factors (41)–(46) in the limit of the infinitely heavy *b* quark mass and large recoil of the final light meson explicitly

satisfy all symmetry relations [6,7] imposed by the large-energy effective theory.

In order to increase the precision and reliability of our calculations compared to our previous consideration [10] we do not perform a further expansion of form factors in inverse powers of the heavy quark mass. Moreover, the q^2 dependence of form factors is explicitly determined by these formulas and thus no *ad hoc* parametrization is necessary. We also use the numerical wave functions found in the meson mass spectrum calculations [11,12] instead of trial (Gaussian) wave functions used in Ref. [10]. To check the precision of the extrapolation of the form factors in the region of small recoil of the final light meson ($\Delta = 0$, $q^2 = q^2_{max}$) we perform the additional consideration of form factors in this region. In this analysis the simplifying substitution of the light quark energy $\epsilon_q(p) = \sqrt{p^2 + m_q^2}$ by the on-shell center of mass energy $E_q = (M^2 - m_Q^2 + m_q^2)/(2M)$ (3) in the contribution of the vertex function $\Gamma^{(2)}$ is used. Such a replacement is valid in the small region around the zero recoil point. As a result in this point one gets expressions for the form factors similar to the formulas given in the appendix of Ref. [38] with obvious substitutions. Such calculation showed that the obtained values of form factors for semileptonic decays $B \to (\pi, \rho)e\nu$ as well as their slopes at zero recoil $q^2 = q^2_{max}$ are in good agreement with the results found from the extrapolation of Eqs. (41)–(46). The deviations are less than 1% confirming the reliability of such extrapolation and of final results which are based on it.

The semileptonic $B \to (\pi, \rho)e\nu$ decay form factors in our model can be approximated with good accuracy by the following expressions [35]:

(a) $F(q^2) = f_+(q^2), V(q^2), A_0(q^2)$

$$F(q^2) = \frac{F(0)}{(1 - \frac{q^2}{\tilde{M}^2})(1 - \sigma_1 \frac{q^2}{M_{B^*}^2} + \sigma_2 \frac{q^4}{M_{B^*}^4})}, \quad (47)$$

(b) $F(q^2) = A_1(q^2), A_2(q^2)$

$$F(q^2) = \frac{F(0)}{(1 - \sigma_1 \frac{q^2}{M_{B^*}^2} + \sigma_2 \frac{q^4}{M_{B^*}^4})}, \quad (48)$$

where $\tilde{M} = M_B$ for A_0 and $\tilde{M} = M_{B^*}$ for all other form factors; the values $F(0)$ and $\sigma_{1,2}$ are given in Table III. The difference of fitted form factors from the calculated ones does not exceed 1%.

In Table IV we give a comparison of the predictions for the form factors of semileptonic decays $B \to (\pi, \rho)e\nu$ at maximum recoil point $q^2 = 0$, calculated in our model with the results of light cone QCD sum rules (LCSR) [39–41], the quark model (QM) [35], using relativistic dispersion relations and two recent lattice QCD (LQCD) calculations [42,43] with dynamical light quarks. Note that

TABLE III. Form factors of semileptonic decays $B \to (\pi, \rho)e\nu$ calculated in our model. Form factors $f_+(q^2)$, $V(q^2)$, $A_0(q^2)$ are fitted by Eq. (47), and form factors $A_1(q^2)$, $A_2(q^2)$ are fitted by Eq. (48).

| | $B \to \pi$ | | $B \to \rho$ | | | |
	f_+	f_0	V	A_0	A_1	A_2
$F(0)$	0.217	0.217	0.295	0.231	0.269	0.282
σ_1	0.378	−0.501	0.875	0.796	0.54	1.34
σ_2	−0.41	−1.50	0	−0.055	0	0.21

our new results for form factors at this point coincide with previous calculations [10] within errors caused by the Gaussian parametrization of the heavy-light meson wave functions used in Ref. [10]. In Ref. [44] a model independent constraint for the product $|V_{ub}|f_+(0) = (7.2 \pm 1.8) \times 10^{-4}$ was obtained using the soft-collinear effective theory and $B \to \pi\pi$ data, which for their final value of $|V_{ub}|$ yields $f_+(0) = 0.227 \pm 0.047$.

The q^2 form factor dependence is plotted in Figs. 8 and 9. In Fig. 8 we also show recent lattice results for the form factors $f_+(q^2)$ and $f_0(q^2)$ [42,43]. It is clearly seen from this figure that the behavior of the form factor $f_+(q^2)$ agrees with lattice computations within errors, while our form factor $f_0(q^2)$ lies somewhat lower than lattice data. In this figure we also show the LCSR result for the value of form factors at $q^2 = 0$ [39]. It agrees with our model prediction within errors.

We can also check the consistency of the obtained q^2 behavior of the form factor f_+ by comparing its calculated value at q^2_{max} with model independent results of chiral perturbation theory (ChPT). For the pion recoil energy $E_\pi \sim m_\pi$ ChPT predicts [44]

$$f_+(q^2(E_\pi)) = \frac{g f_B M_B}{2 f_\pi(E_\pi + M_{B^*} - M_B)}\left[1 + O\left(\frac{E_\pi}{\Delta}\right)\right], \quad (49)$$

where $g \sim 0.5$ is $B^* B \pi$ coupling [44], the decay constant f_B is equal to 189 MeV in our model [45]. The first corrections scale as E_π/Δ, where $\Delta \sim 600$ MeV is the mass splitting to the first radially excited 1^- state above the B^*. Substituting these values one gets the following prediction [44]

$$f_+(q^2_{max}) = 10.38 \pm 3.63, \quad (50)$$

which is in agreement with our model result $f_+(q^2_{max}) = 10.9$.

On the other hand, the form factor f_0 in the soft-pion limit $p \to 0$ and $m_\pi^2 \to 0$ is related to the ratio of the B and π decay constants [39,46]

$$f_0(q^2_{max}) = \frac{f_B}{f_\pi}. \quad (51)$$

This relation with the above values of the decay constants

TABLE IV. Comparison of theoretical predictions for the form factors of semileptonic decays $B \to (\pi, \rho)e\nu$ at maximum recoil point $q^2 = 0$.

	$f_+(0)$	$V(0)$	$A_0(0)$	$A_1(0)$	$A_2(0)$
Our	0.217	0.295	0.231	0.269	0.282
LCSR [39,40]	0.258(31)	0.323(29)	0.303(28)	0.242(24)	0.221(23)
LCSR [41]	0.25(5)	0.32(10)		0.24(8)	0.21(9)
QM [35]	0.29	0.31	0.29	0.26	0.24
QM [10]	0.20(2)	0.29(3)		0.26(3)	0.31(3)
LQCD(FNAL)[42]	0.23(2)				
LQCD(HPQCD)[43]	0.27(5)				

gives the result $f_0(q^2_{\max}) = 1.45$ again in good agreement with the prediction of our model $f_0(q^2_{\max}) = 1.36$.

The differential semileptonic decay rates can be expressed in terms of these form factors by

(i) $B \to Pe\nu$ decay ($P = \pi$)

$$\frac{d\Gamma}{dq^2}(B \to Pe\nu) = \frac{G_F^2 \Delta^3 |V_{qb}|^2}{24\pi^3} |f_+(q^2)|^2. \quad (52)$$

(ii) $B \to Ve\nu$ decay ($V = \rho$)

$$\frac{d\Gamma}{dq^2}(B \to Ve\nu) = \frac{G_F^2 \Delta |V_{qb}|^2}{96\pi^3} \frac{q^2}{M_B^2}(|H_+(q^2)|^2 \\ + |H_-(q^2)|^2 + |H_0(q^2)|^2), \quad (53)$$

where G_F is the Fermi constant, V_{qb} is the CKM matrix element ($q = u$),

$$\Delta \equiv |\boldsymbol{\Delta}| = \sqrt{\frac{(M_B^2 + M_{P,V}^2 - q^2)^2}{4M_B^2} - M_{P,V}^2}.$$

Helicity amplitudes are given by the following expressions

$$H_{\pm}(q^2) = \frac{2M_B\Delta}{M_B + M_V}\left[V(q^2) \mp \frac{(M_B + M_V)^2}{2M_B\Delta} A_1(q^2)\right], \quad (54)$$

$$H_0(q^2) = \frac{1}{2M_V\sqrt{q^2}}\left[(M_B + M_V)(M_B^2 - M_V^2 - q^2)A_1(q^2) \\ - \frac{4M_B^2\Delta^2}{M_B + M_V}A_2(q^2)\right]. \quad (55)$$

The decay rates in transversally and longitudinally polarized vector mesons are defined by

$$\frac{d\Gamma_L}{dq^2} = \frac{G_F^2\Delta |V_{qb}|^2}{96\pi^3}\frac{q^2}{M_B^2}|H_0(q^2)|^2, \quad (56)$$
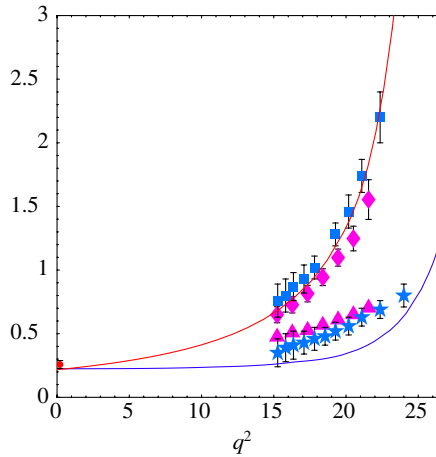
FIG. 8 (color online). Form factors of the semileptonic decay $B \to \pi e\nu$ in comparison with lattice calculations: $f_+(q^2)$ is given by the upper plot (our), squares (FNAL) [42], diamonds (HPQCD) [43]; $f_0(q^2)$ is given by the lower plot (our), stars (FNAL) [42], triangles (HPQCD) [43]. The LCSR value for from factors at $q^2 = 0$ is plotted by a circle [39].
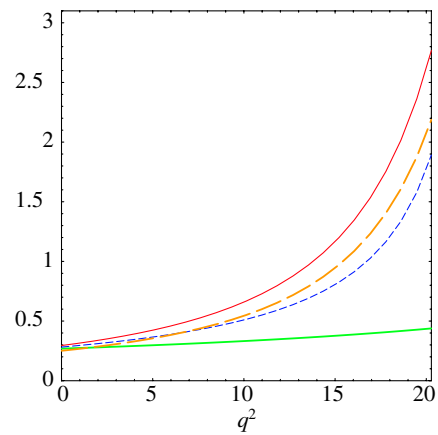
FIG. 9 (color online). Form factors of the semileptonic decay $B \to \rho e\nu$: $V(q^2)$ is plotted by the solid line, $A_1(q^2)$—by the bold line, $A_2(q^2)$—by dashed line, and $A_0(q^2)$—by long-dashed line.

TABLE V. Comparison of theoretical predictions for the rates of semileptonic decays $B \to (\pi, \rho)e\nu$ (in $|V_{ub}|^2$ ps^{-1}).

Decay	Our	Γ LCSR [39]	FNAL [42]	HPQCD [43]	$\Gamma^{q^2<16 \text{ GeV}^2}$ Our	LCSR [39]	$\Gamma^{q^2>16 \text{ GeV}^2}$ Our	FNAL [42]	HPQCD [43]
$B \to \pi e\nu$	5.45	7.74(2.32)	6.24(2.12)	6.03(1.94)	3.68	5.44(1.43)	1.77	1.83(50)	1.46(35)
$B \to \rho e\nu$	13.1				10.5		2.60		

$$\frac{d\Gamma_T}{dq^2} = \frac{d\Gamma_+}{dq^2} + \frac{d\Gamma_-}{dq^2}$$
$$= \frac{G_F^2 \Delta |V_{qb}|^2}{96\pi^3} \frac{q^2}{M_B^2} (|H_+(q^2)|^2 + |H_-(q^2)|^2). \quad (57)$$

Integration over q^2 of these formulas gives the total rate of the corresponding semileptonic decay. These rates are presented in Table V. In this table we also give the values of the partial decay rates integrated over two intervals $q^2 < 16$ GeV^2 and $q^2 > 16$ GeV^2 in comparison with the evaluations of LCSR in the first interval and LQCD in the second interval [47]. This is related to the fact that the predictions of these approaches are reliable only in the above mentioned regions. The results presented in Table V show that our calculations agree well with the lattice evaluations, while our values are somewhat lower than LCSR ones which have relatively large errors. Note that our model gives the ratio of semileptonic B decay rates into ρ meson with longitudinal polarization to the corresponding rate with transverse polarization $\Gamma_L/\Gamma_T = 0.46$.

Using mean lifetimes of B mesons [37]: $\tau_{B^0} = 1.530 \times 10^{-12}$ s and $\tau_{B^+} = 1.671 \times 10^{-12}$ s, we find

$$\text{BR}(B^0 \to \pi^+ l^- \nu) = 8.34|V_{ub}|^2,$$
$$\text{BR}(B^+ \to \pi^0 l^+ \nu) = 4.47|V_{ub}|^2,$$
$$\text{BR}(B^0 \to \rho^+ l^- \nu) = 20.1|V_{ub}|^2, \quad (58)$$
$$\text{BR}(B^+ \to \rho^0 l^+ \nu) = 10.7|V_{ub}|^2.$$

Comparison of these predictions with experimental data [37] leads to the following values of $|V_{ub}|$:

$$\text{BR}(B^0 \to \pi^+ l^- \nu)^{\text{exp}} = (1.36 \pm 0.15) \times 10^{-4}$$
$$|V_{ub}| = (4.04 \pm 0.25) \times 10^{-3},$$
$$\text{BR}(B^+ \to \pi^0 l^+ \nu)^{\text{exp}} = (7.4 \pm 1.1) \times 10^{-4}$$
$$|V_{ub}| = (4.07 \pm 0.30) \times 10^{-3},$$
$$\text{BR}(B^0 \to \rho^+ l^- \nu)^{\text{exp}} = (2.3 \pm 0.4) \times 10^{-4} \quad (59)$$
$$|V_{ub}| = (3.38 \pm 0.30) \times 10^{-3},$$
$$\text{BR}(B^+ \to \rho^0 l^+ \nu)^{\text{exp}} = (1.24 \pm 0.23) \times 10^{-4}$$
$$|V_{ub}| = (3.39 \pm 0.33) \times 10^{-3}.$$

Decays of the neutral and charged B mesons give very close results for $|V_{ub}|$, while the averaged values of $|V_{ub}|$, extracted form the decay $B \to \rho e\nu$ are approximately 16% lower than corresponding values, found from the decay

$B \to \pi e\nu$. Note that the recent CLEO [48] measurement of the decay branching ratio BR$(B^0 \to \rho^+ l^- \nu)^{\text{exp}} = (2.91 \pm 0.54) \times 10^{-4}$ gives $|V_{ub}| = (3.81 \pm 0.35) \times 10^{-3}$ which is close to the one extracted from the $B \to \pi e\nu$ decay.

Recently significant progress has been achieved in the experimental determination of the differential decay $B \to (\pi, \rho)e\nu$ rate dependence on q^2. CLEO [48,49], *BABAR* [50–52], and Belle [53] measured partial decay rates in relatively narrow intervals of q^2. In Figs. 10 and 11 we present the comparison of our model predictions for partial branching ratios of $B \to (\pi, \rho)e\nu$ decays with experimental data. Plotting histograms in Figs. 10(a)–10(c), 11(a), and 11(b) we used the value of $|V_{ub}|$, extracted from the total rate in the corresponding experiments. It is clearly seen that our predictions agree well with almost all data for
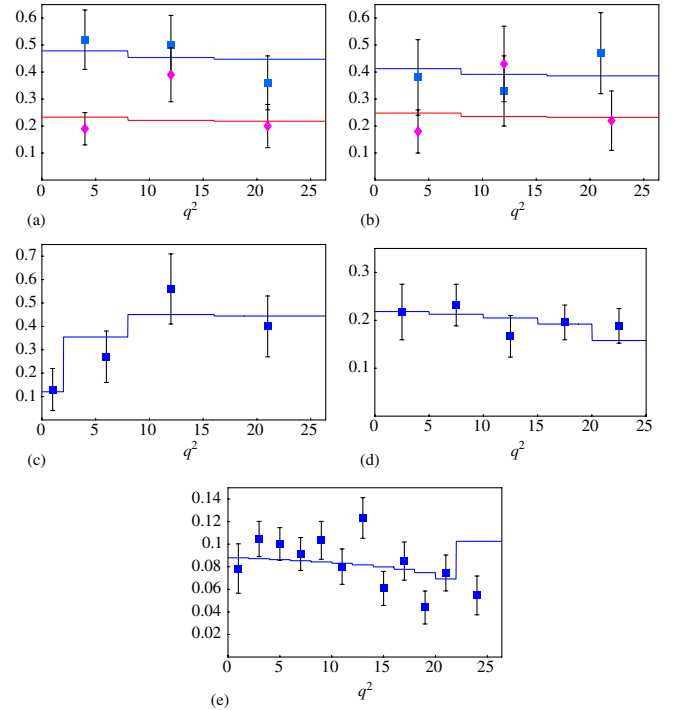
FIG. 10 (color online). Comparison of theoretical predictions for partial decay rates with experimental data: (a)–(c) $(1/\Gamma_{\text{tot}})(\int_{\Delta q^2}(d\Gamma(B \to \pi e\nu)/dq^2)dq^2) \times 10^4$ from Refs. [48,50,53]; (d), (e) $\Delta\text{BR}(B \to \pi e\nu)/\text{BR}(B \to \pi e\nu)$ from Refs. [51,52], respectively. Lower histograms on (a), (b) and diamonds are theoretical and experimental values for decays of the charged B meson $B^+ \to \pi^0 e^+ \nu$. All other histograms and squares are theoretical predictions and experimental data for decays of the neutral B meson $B^0 \to \pi^+ e^- \nu$.
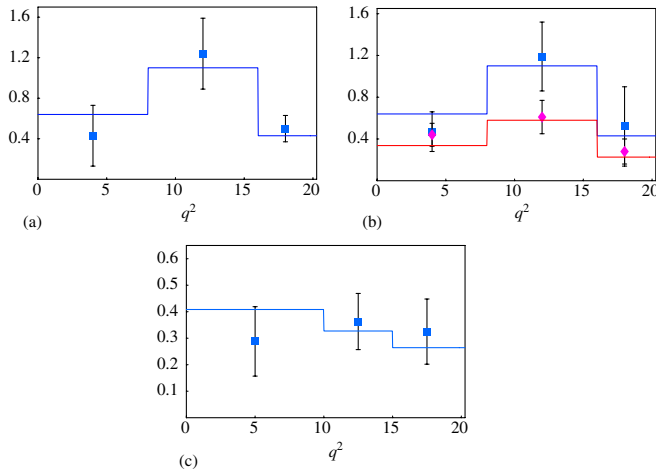
FIG. 11 (color online). Comparison of theoretical predictions for partial decay rates with experimental data: (a), (b) $(1/\Gamma_{\text{tot}})(\int_{\Delta q^2}(d\Gamma(B \to \rho e\nu)/dq^2)dq^2) \times 10^4$ from Refs. [49,53]; (c) $\Delta\text{BR}(B \to \rho e\nu)/\text{BR}(B \to \rho e\nu)$ from Ref. [51], respectively. Lower histograms on (b) and diamonds are theoretical and experimental values for decays of the charged B meson $B^+ \to \rho^0 e^+\nu$. All other histograms and squares are theoretical predictions and experimental data for decays of the neutral B meson $B^0 \to \rho^+ e^-\nu$.

decays of neutral as well as charged B mesons. Using these experimental data on partial and total semileptonic $B \to (\pi, \rho)e\nu$ decay rates it is possible to extract averaged values of $|V_{ub}|$:

$$
\begin{aligned}
B \to \pi e\nu \qquad & |V_{ub}| = (4.02 \pm 0.10) \times 10^{-3}, \\
B \to \rho e\nu \qquad & |V_{ub}| = (3.33 \pm 0.20) \times 10^{-3},
\end{aligned}
\tag{60}
$$

which are in good agreement with the ones, extracted from averaged total decay rates (59).

Finally, averaging over all above mentioned experimental data we get the value of $|V_{ub}|$ in our model

$$
|V_{ub}| = (3.82 \pm 0.20) \times 10^{-3}
\tag{61}
$$

in good agreement with PDG [37]

$$
|V_{ub}| = (3.84^{+0.67}_{-0.49}) \times 10^{-3} \qquad \text{(exclusive)}.
$$

VI. CONCLUSION

We calculated weak decay form factors and decay rates of different semileptonic B decays. Decays both into heavy $D^{(*)}$ and light $\pi(\rho)$ mesons were considered.

First, it was shown that our relativistic quark model gives a reliable description of the heavy-to-heavy semileptonic transitions $B \to D^{(*)}l\nu$. All model independent HQET relations are reproduced. The model allows to express corresponding leading and subleading order Isgur-Wise functions through overlap integrals of meson wave functions. These wave functions were determined previously in the process of the meson mass spectrum calcula-

tions. From the comparison with the experiment and predictions of other theoretical approaches it follows that our model correctly reproduces the q^2 behavior of form factors. Calculated decay rates and branching fractions are in good agreement with data and give very close values of the CKM matrix element $|V_{cb}|$ extracted from different decay processes.

Second, the form factors of the heavy-to-light semileptonic B decays were calculated. The consideration was done with the systematic treatment of all relativistic effects, which are very important for such transitions. Particular attention was paid to the inclusion of negative-energy contributions and to the relativistic transformation of the meson wave function from the rest to the moving reference frame. The q^2 dependence of the form factors was explicitly determined without using any *ad hoc* assumptions. The validity of the form factor extrapolation, which is necessary only within the small region near the point of zero recoil of the final light meson, was cross-checked by an additional calculation of the form factor values in this particular point. The decay form factors are again given by the overlap integrals of the B and π, ρ meson wave functions, which are known from the previous calculations of the meson mass spectra. The q^2 behavior of the form factors is in agreement with both unquenched lattice QCD calculations and predictions of light cone QCD sum rules within the ranges of the validity of these approaches. All this significantly improves the reliability of the obtained results. The comprehensive comparison of the predictions with recent experimental data both on total and partial decay rates allowed the extractions of the CKM matrix element $|V_{ub}|$ which values are rather close in different decay channels.

The evaluation of the theoretical uncertainties represents an important problem. Unfortunately, it is not easy to estimate them in the framework of the adopted approach. The theoretical errors within the model, which come from the neglected higher order terms in the $1/m_Q$ expansion for heavy-to-heavy transitions and from the form factor extrapolation in the region of zero recoil for heavy-to-light transitions, can be easily estimated and are less than 3%. The main difficulty is related to the uncertainty of the quark model itself. However, our previous experience in calculating a vast set of different properties of hadrons within our model indicates that such uncertainties should not exceed 5%.[1] Therefore, adding these errors in quad-

---

[1]The model parameters were fixed in previous studies through fitting the experimental data. The integrated quantities such as semileptonic decay rates are much less sensitive to the variation of the model parameters than such quantities as hadron masses which are measured with considerably higher accuracy. Thus even the limited variation of these parameters, permitted by the description of hadron masses, will give significantly smaller contributions to the decay-rate and CKM matrix-element uncertainties compared to the ones mentioned above.

rature we find for the CKM matrix elements the following final values in our model:

$$|V_{cb}| = (3.85 \pm 0.15 \pm 0.20) \times 10^{-2},$$
$$|V_{ub}| = (3.82 \pm 0.20 \pm 0.20) \times 10^{-3}, \tag{62}$$

where the first error is experimental and the second one is theoretical. Since the presented determination of $|V_{cb}|$ and $|V_{ub}|$ is model dependent we do not pretend that this

determination is more reliable than others (e.g. the lattice one or from QCD sum rules).

[1] R. V. Kowalewski, hep-ex/0610059.
[2] N. Isgur and M. B. Wise, Phys. Lett. B **232**, 113 (1989); **237**, 527 (1990).
[3] N. Isgur and M. B. Wise, Phys. Rev. D **43**, 819 (1991).
[4] M. Neubert, Phys. Rep. **245**, 259 (1994); Int. J. Mod. Phys. A **11**, 4173 (1996).
[5] M. J. Dugan and B. Grinstein, Phys. Lett. B **255**, 583 (1991).
[6] J. Charles *et al.*, Phys. Rev. D **60**, 014001 (1999).
[7] D. Ebert, R. N. Faustov, and V. O. Galkin, Phys. Rev. D **64**, 094022 (2001).
[8] R. N. Faustov and V. O. Galkin, Z. Phys. C **66**, 119 (1995).
[9] R. N. Faustov, V. O. Galkin, and A. Yu. Mishurov, Phys. Rev. D **53**, 1391 (1996).
[10] R. N. Faustov, V. O. Galkin, and A. Yu. Mishurov, Phys. Rev. D **53**, 6302 (1996).
[11] D. Ebert, V. O. Galkin, and R. N. Faustov, Phys. Rev. D **57**, 5663 (1998); **59**, 019902(E) (1999).
[12] D. Ebert, R. N. Faustov, and V. O. Galkin, Mod. Phys. Lett. A **20**, 1887 (2005); Eur. Phys. J. C **47**, 745 (2006).
[13] A. A. Logunov and A. N. Tavkhelidze, Nuovo Cimento **29**, 380 (1963).
[14] A. P. Martynenko and R. N. Faustov, Teor. Mat. Fiz. **64**, 179 (1985) [Theor. Math. Phys. (Engl. Transl.) **64**, 765 (1985)].
[15] V. O. Galkin, A. Yu. Mishurov, and R. N. Faustov, Yad. Fiz. **55**, 2175 (1992) [Sov. J. Nucl. Phys. **55**, 1207 (1992)].
[16] D. Ebert, R. N. Faustov, and V. O. Galkin, Phys. Rev. D **62**, 034014 (2000); **67**, 014027 (2003).
[17] E. Eichten and F. Feinberg, Phys. Rev. D **23**, 2724 (1981).
[18] V. O. Galkin and R. N. Faustov, Yad. Fiz. **44**, 1575 (1986) [Sov. J. Nucl. Phys. **44**, 1023 (1986)]; D. Ebert, R. N. Faustov, and V. O. Galkin, Phys. Lett. B **537**, 241 (2002).
[19] H. J. Schnitzer, Phys. Rev. D **18**, 3482 (1978).
[20] R. N. Faustov, Ann. Phys. (N.Y.) **78**, 176 (1973); Nuovo Cimento A **69**, 37 (1970).
[21] M. E. Luke, Phys. Lett. B **252**, 447 (1990).
[22] K. C. Bowler *et al.* (UKQCD Collaboration), Nucl. Phys. **B637**, 293 (2002).
[23] A. Le Yaouanc, L. Oliver, and J. C. Raynal, Phys. Rev. D **69**, 094022 (2004).
[24] S. Hashimoto, A. X. El-Khadra, A. S. Kronfeld, P. B. Mackenzie, S. M. Ryan, and J. N. Simone, Phys. Rev. D **61**, 014502 (1999).
[25] I. Caprini, L. Lellouch, and M. Neubert, Nucl. Phys. **B530**, 153 (1998).
[26] J. Bartelt *et al.* (CLEO Collaboration), Phys. Rev. Lett. **82**, 3746 (1999).
[27] K. Abe *et al.* (BELLE Collaboration), Phys. Lett. B **526**, 258 (2002).
[28] C. G. Boyd, B. Grinstein, and R. F. Lebed, Phys. Rev. D **56**, 6895 (1997).
[29] S. Hashimoto, A. S. Kronfeld, P. B. Mackenzie, S. M. Ryan, and J. N. Simone, Phys. Rev. D **66**, 014503 (2002).
[30] B. Grinstein and Z. Ligeti, Phys. Lett. B **526**, 345 (2002).
[31] N. E. Adam *et al.* (CLEO Collaboration), Phys. Rev. D **67**, 032001 (2003).
[32] B. Aubert *et al.* (*BABAR* Collaboration), Phys. Rev. D **71**, 051502 (2005); Phys. Rev. D **74**, 092004 (2006).
[33] K. Abe *et al.* (BELLE Collaboration), Phys. Lett. B **526**, 247 (2002).
[34] J. Abdallah *et al.* (DELPHI Collaboration), Eur. Phys. J. C **33**, 213 (2004).
[35] D. Melikhov and B. Stech, Phys. Rev. D **62**, 014006 (2000).
[36] C. Albertus, E. Hernandez, J. Nieves, and J. M. Verde-Velasco, Phys. Rev. D **71**, 113006 (2005).
[37] W.-M. Yao *et al.* (Particle Data Group), J. Phys. G **33**, 1 (2006).
[38] D. Ebert, R. N. Faustov, and V. O. Galkin, Eur. Phys. J. C **32**, 29 (2003).
[39] P. Ball and R. Zwicky, Phys. Rev. D **71**, 014015 (2005).
[40] P. Ball and R. Zwicky, Phys. Rev. D **71**, 014029 (2005).
[41] A. Khodjamirian, T. Mannel, and N. Offen, Phys. Rev. D **75**, 054013 (2007).
[42] M. Okamoto *et al.* (FNAL Collaboration), Nucl. Phys. B, Proc. Suppl. **140**, 461 (2005).
[43] E. Gulez *et al.* (HPQCD Collaboration), Phys. Rev. D **73**, 074502 (2006).
[44] C. M. Arnesen, B. Grinstein, I. Z. Rothstein, and I. W. Stewart, Phys. Rev. Lett. **95**, 071802 (2005).
[45] D. Ebert, R. N. Faustov, and V. O. Galkin, Phys. Lett. B **635**, 93 (2006).
[46] M. B. Voloshin, Yad. Fiz. **50**, 166 (1989) [Sov. J. Nucl. Phys. **50**, 105 (1989)].
[47] Heavy Flavor Averaging Group (HFAG), hep-ex/0603003.

[48] Y. Gao (CLEO Collaboration), in Proceedings of the ICHEP, Moscow, Russia, 2006 (unpublished).

[49] S. B. Athar *et al.* (CLEO Collaboration), Phys. Rev. D **68**, 072003 (2003).

[50] B. Aubert *et al.* (*BABAR* Collaboration), Phys. Rev. Lett. **97**, 211801 (2006).

[51] B. Aubert *et al.* (*BABAR* Collaboration), Phys. Rev. D **72**, 051102 (2005).

[52] B. Aubert *et al.* (*BABAR* Collaboration), hep-ex/0607060.

[53] K. Hokuue *et al.* (BELLE Collaboration), hep-ex/0604024.